

## Exploration of Novel Aryl Binding Sites of Farnesyltransferase Using Molecular Modeling and Benzophenone-Based Farnesyltransferase Inhibitors

Markus Böhm,<sup>#</sup> Andreas Mitsch,<sup>#</sup> Pia Wissner,<sup>#</sup> Isabel Sattler,<sup>§</sup> and Martin Schlitzer<sup>\*,#</sup>

*Institut für Pharmazeutische Chemie, Philipps-Universität Marburg, Marbacher Weg 6, D-35032 Marburg, Germany, and Hans-Knöll-Institut für Naturstoff-Forschung e. V., Beutenbergstrasse 11, D-07745 Jena, Germany*

Received March 7, 2001

Most non-thiol CAAX-peptidomimetic farnesyltransferase inhibitors bear nitrogen-containing heterocycles in place of the terminal cysteine which are supposed to coordinate the enzyme-bound zinc. However, it has been shown that those nitrogen-containing heterocycles can be replaced by carbocyclic aromatic moieties which are unable to coordinate the zinc ion, a conclusion that resulted in the postulation of one or two hitherto unknown aryl binding sites. No indication has been given about the spatial location of these novel binding sites. Employing flexible docking of several non-thiol farnesyltransferase inhibitors known from the literature and some model compounds based on our benzophenone scaffold as well as performing GRID searches, we have identified two regions in the farnesyltransferase's active site which we suggest being the postulated aryl binding sites. One aryl binding region is located in close proximity to the zinc ion and is defined by the aromatic side chains of Tyr 300 $\beta$ , Trp 303 $\beta$ , Tyr 361 $\beta$ , and Tyr 365 $\beta$ . The second aryl binding site is defined by the side chains of Tyr 300 $\beta$ , Leu 295 $\beta$ , Lys 294 $\beta$ , Lys 353 $\beta$ , and Lys 356 $\beta$ . This second aryl binding site has been used for the design of a non-thiol farnesyltransferase inhibitor (**9c**) with an IC<sub>50</sub> of 35 nM.

Inhibition of farnesyltransferase has received considerable interest in recent years as a strategy for the development of novel potential cancer drugs.<sup>1–3</sup> Farnesyltransferase catalyzes the transfer of a farnesyl residue from farnesylpyrophosphate to the thiol of a cysteine side chain of protein bearing the CAAX-tetrapeptide sequence (C: cysteine, A: aliphatic amino acid, X: serine or methionine) at its C-terminus.<sup>4</sup> The rationale for using inhibitors of farnesyltransferase as anticancer agents results from the observation that farnesylation is a prerequisite for the transforming activity of oncogenic Ras, found in approximately 30% of all cancers in humans. However, there is accumulating evidence that prevention of Ras farnesylation may not be the crucial cellular event responsible for the antiproliferative effect of farnesyltransferase inhibitors.<sup>5</sup> Focus has shifted to RhoB, another member of the class of small GTPases which is involved in receptor trafficking.<sup>6,7</sup> Irrespective of the unresolved issue of mechanism by which farnesyltransferase inhibitors exert their antiproliferative effects, the efficacy of these compounds and their low toxicity has been demonstrated,<sup>8</sup> and therefore, administration of such compounds is regarded as a major strategy emerging in cancer therapy.

Most inhibitors described in the literature are peptidomimetics resembling the CAAX-tetrapeptide recognition sequence of farnesylated proteins. The majority of these CAAX-peptidomimetics exhibit a free thiol group<sup>1–3</sup> which is believed to coordinate the enzyme-bound zinc ion as shown for the native peptide substrate.<sup>9</sup> However, free thiols are associated with several adverse drug

effects,<sup>10</sup> and thus the development of farnesyltransferase inhibitors is clearly directed toward the so-called non-thiol farnesyltransferase inhibitors. Most frequently used replacements for cysteine are nitrogen-containing heterocycles. The ring nitrogen is supposed to coordinate to the enzyme-bound zinc similarly to the cysteine thiol group.<sup>11</sup> However, it has been shown that nitrogen heterocycles can be replaced by aryl residues lacking the ability to coordinate metal atoms without losing too much of their farnesyltransferase inhibitory activity.<sup>12,13</sup> Therefore, the existence of at least one hitherto unknown aryl binding region in the farnesyltransferase's active site has been postulated.<sup>14,15</sup> Until now, no evidence has been provided for the spatial location of this postulated aryl binding site in the farnesyltransferase's active site.

We intended to address this issue using flexible docking methods of both representative non-thiol farnesyltransferase inhibitors known from literature<sup>12–14,16</sup> (Chart 1) as well as some model compounds based on our benzophenone AAX-peptidomimetic scaffold.<sup>17,18</sup> In addition, we performed GRID analyses searching for regions favorable for aryl binding. Using these molecular modeling studies, we are able to provide a reasonable suggestion about the location of the above-mentioned postulated aryl binding regions in the farnesyltransferase's active site.

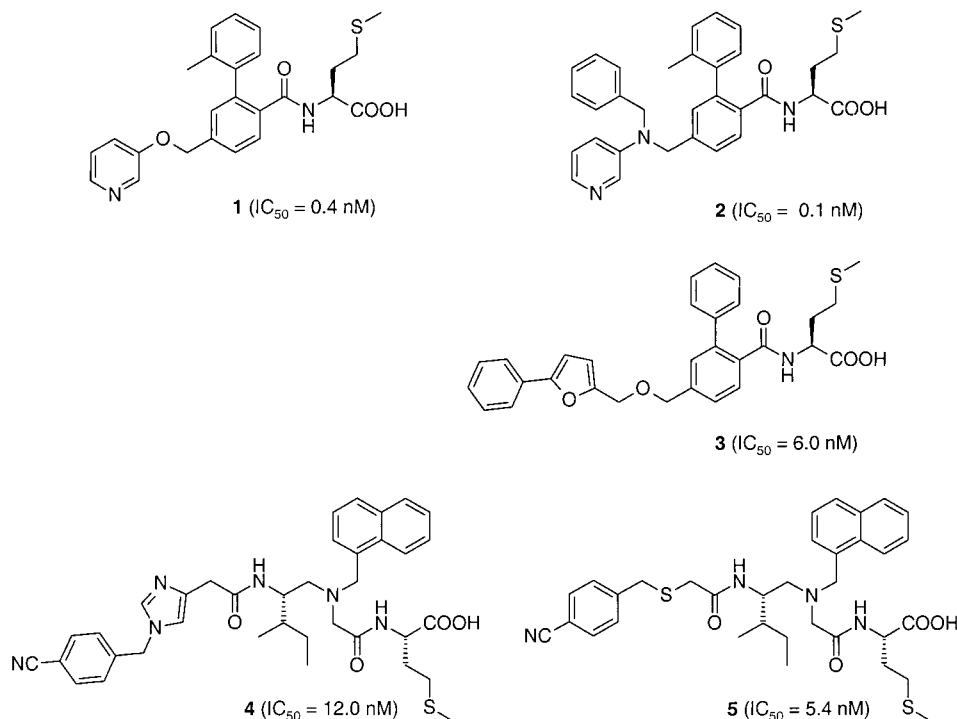
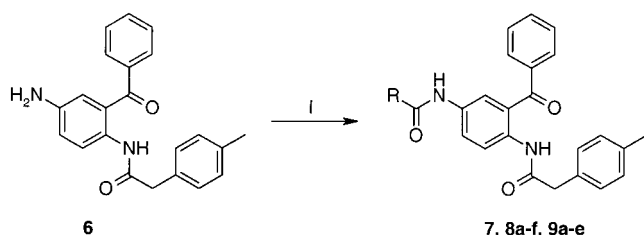
### Chemistry

The *p*-tolylacetyl-amino-5-aminobenzophenone scaffold **6** has been prepared,<sup>19</sup> as described, in two steps from commercially available starting material. Compound **6** was acylated by appropriate acyl chlorides in hot toluene to yield the target compounds **7**, **8a–f**, and **9a–e** (Scheme 1).

\* To whom correspondence should be addressed. Phone: +49 6421 2825825. Fax: +49 6421 2827052. E-mail: schlitze@mail.uni-marburg.de.

<sup>#</sup> Universität Marburg.

<sup>§</sup> Hans-Knöll-Institut für Naturstoff-Forschung.

**Chart 1.** Structures and Activities of Representative Non-Thiol Farnesyltransferase Inhibitors Described in the Literature That Were Used for Flexible Docking**Scheme 1<sup>a</sup>**

<sup>a</sup> (I) R-COCl, toluene or toluene/dioxane, reflux, 2 h.

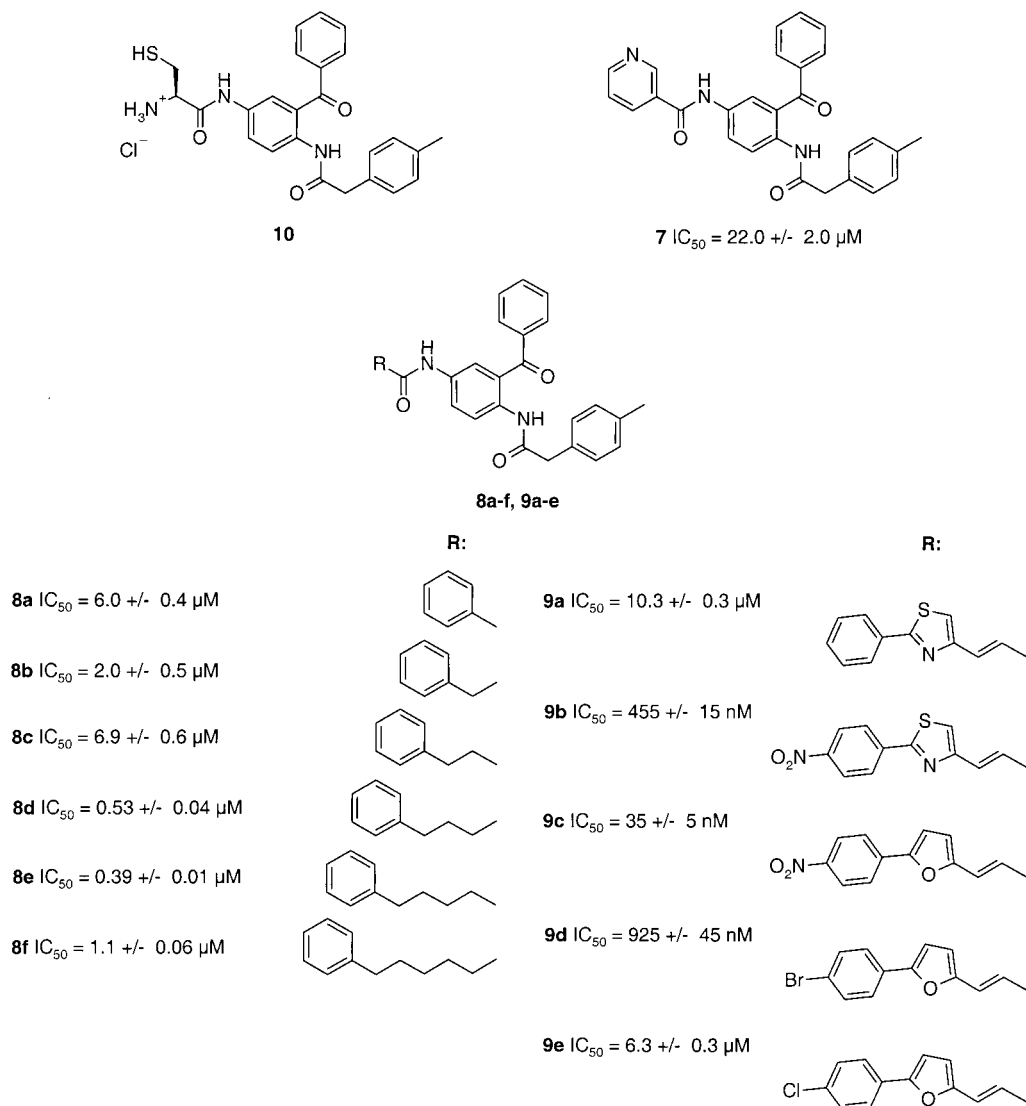
**Flexible Docking**

Flexible docking of both non-thiol farnesyltransferase inhibitors **1–5** known from literature<sup>12–14,16</sup> (Chart 1) as well as the model compounds **8b** and **8e** (Chart 2) was performed using the program FlexX.<sup>20</sup> On the basis of the coordinates of the published crystal structure<sup>9</sup> of a ternary complex of farnesyltransferase, a farnesylpyrophosphate analogue and *N*-acetyl-Cys-Val-Ile-selenoMetOH (PDB-code 1QBQ), we have calculated the solvent accessible surface of the farnesyltransferase's active site using the program MOLCAD which is implemented in the molecular modeling software package SYBYL.<sup>21</sup> Due to our working hypothesis, the postulated aryl binding sites should be located next to the peptide binding region. Thus, we included the farnesylpyrophosphate as part of the enzyme's molecular surface. The position of the HOOC-CH<sub>α</sub>-NH-moiety of the CAAX-peptide as found in the crystal structure was used as a starting fragment for the docking of inhibitors **1–5** into the farnesyltransferase's active site. Subsequently, the docking program places the remaining fragments of the inhibitors in a piece-wise fashion into the active site searching for favorable hydrophobic and H-bond interactions while avoiding steric overlaps.

In case of the model compounds **8b** and **8e**, the tolyl-OC-NH-moiety was assumed to be isosteric to the HOOC-C<sub>α</sub>H-NH- fragment of the CAAX-peptide<sup>18</sup> and was therefore used as the starting fragment. The docking runs provided sets of solutions which were inspected according to their suggested binding energy. Obviously unreasonable solutions were excluded, for instance, those where major parts of the inhibitors were exposed merely to the solvent without showing specific interactions within the active site.

**GRID Analysis**

The program GRID<sup>22–25</sup> allows the identification of regions of energetically favorable interactions between a molecule and a probe. It can therefore be applied to detect those regions in a protein's active site which are important for the binding of partial structures with certain physicochemical properties. A three-dimensional grid is placed in the active site large enough to encompass all residues relevant for protein–ligand interaction. At each grid node, interaction energies between a specific probe and all atoms of the target (binding site of farnesyltransferase) are calculated. Depending upon which chemical information is desired, GRID allows different types of probes to be used which are specific for a certain atom or fragment. Here we utilized the “C1=” probe (sp<sup>2</sup> CH aromatic moiety) to detect favorable positions for aromatic binding. As some of our highly potent benzophenone-based inhibitors contain a nitro group, the “ON” probe can highlight those regions favorable for oxygen atoms of a nitro group. In contrast, ligands containing a bromine or chlorine substituent at the same position as the nitro group show a reduced inhibitory activity. Therefore, inspecting the interaction energies derived from the “CL” (chlorine) probe, for instance, can help to explain this loss of activity.

**Chart 2.** Structures and Activities of Benzophenone-Based Farnesyltransferase Inhibitors

## Results and Discussion

As a first step to embark into the class of non-thiol farnesyltransferase inhibitors based on our benzophenone scaffold, we replaced the terminal cysteinyl residue in our lead structure **10**<sup>18</sup> by a nicotinoyl moiety (**7**). This resulted in a significant loss of activity (**10**:  $IC_{50} = 77 \text{ nM}$ ; **7**:  $IC_{50} = 22 \mu M$ ). With respect to published results,<sup>26</sup> this reduction in activity was not unexpected. The subsequent replacement of the pyridyl by a phenyl ring improved activity (**8a**:  $IC_{50} = 6 \mu M$ ), confirming that the ability to coordinate the enzyme-bound zinc is not mandatory for farnesyltransferase inhibitory activity. This result is also consistent with observations collected by other groups<sup>12,13</sup> and led to the postulation of one or two hitherto unknown aryl binding sites in the farnesyltransferase's active site.<sup>14,15</sup> Considering the improved activity of the carbocycle-containing compound **8a** compared to the nicotinyl derivative **7** and, above all, because making usage of a lipophilic moiety instead of a zinc-coordinating group represents a novel concept in farnesyltransferase inhibitor design, we decided to focus our attention on this type of compounds instead of addressing the effect of different heterocycles such as imidazoles.

To explore these postulated aryl binding sites, we next prepared some model compounds varying the distance between the phenyl residue and the AAX-peptidomimetic benzophenone scaffold by introducing spacer groups with successively increasing numbers of methylene groups between the phenyl ring and the terminal amide moiety (**8b–f**, Chart 2). Introduction of one methylene group in **8a** as in the phenylacetic acid derivative **8b** resulted in a 3-fold improvement in activity. Elongation of the spacer by one additional methylene unit (**8c**) decreased the farnesyltransferase inhibitory activity. Compounds **8d** and **8e** incorporating spacers of three and four methylene units, respectively, display considerably enhanced inhibitory activities with  $IC_{50}$  values in the submicromolar range. Further elongation of the spacer resulted again in a reduction of activity. These results are consistent with the existence of two different aryl binding sites as it has been postulated.<sup>15</sup>

Since no indication has been given about the spatial location of these novel aryl binding sites, we performed some docking experiments using both representative non-thiol farnesyltransferase inhibitors **1–5** known from literature as well as our benzophenone-type inhibi-

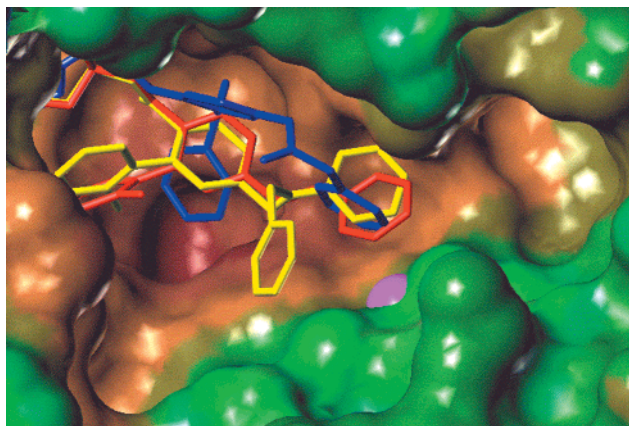


**Figure 1.** Results from docking runs of compounds **1** (red), **2** (yellow), and **8b** (blue) placing the terminal aryl residue into a lipophilic cleft next to the zinc (magenta). Hydrophobic properties of the enzyme's surface are indicated in brown, hydrophilic in green to blue colors. Enzyme-bound zinc is shown as a magenta sphere.

tors **8b** and **8f**. We set forward the working hypothesis that the aryl binding sites should be located next to the peptide binding region in the farnesyltransferase's active site. As most of the compounds seem to be unable to adopt such a strongly bended conformation which would be necessary to fit into the peptide binding site and, at the same time, into the prenyl binding site, it seems appropriate to assume that the farnesyltransferase-farnesylpyrophosphate complex is the target of this type of inhibitor although no kinetic studies were carried out to clearly indicate this assumption. Therefore, farnesylpyrophosphate was integrated into the binding site while computing the protein's molecular surface and performing the docking runs as well as the GRID analyses.

Flexible docking of inhibitors **1**, **2**, and **8b** exposing their terminal aryl moiety in relatively short distance to the center of the molecules resulted in all three cases in sets of solutions showing the aryl residues placed into a lipophilic binding cleft (Figure 1) in close proximity to the enzyme-bound zinc. This binding site ("near") is defined by the aromatic amino acid side chains of Tyr 300 $\beta$ , Trp 303 $\beta$ , Tyr 361 $\beta$ , and Tyr 365 $\beta$  (Figure 3). Hydrophobic interactions of the aryl moieties of **1**, **2**, and **8b** with respect to the first three neighboring amino acid side chains are suggested by FlexX for all three inhibitors. Compounds **3**, **4**, **5**, and **8e** are obviously too large to fit into this binding cleft. In the case of inhibitors **3**, **4**, and **8e**, two alternative solutions are proposed by FlexX. One solution shows the aryl residues bended toward the "southern hemisphere" of farnesyltransferase's active site (Figure 2a). Here a hydrophobic interaction with the phenyl residue of Tyr 361 $\beta$  is found. It should be noted that this interaction formed to the opposite side of the Tyr 361 $\beta$  side chain is different from that seen with the shorter molecules **1**, **2**, and **8b**. In addition, the N-benzyl substituent of compound **2** is placed by FlexX into this region. However, no comparable solution in which the lipophilic residue is placed into this southern region was predicted for compound **5**. In the second subset of reasonable solutions, the aryl moieties of all four inhibitors **3**, **4**, **5**, and **8e** are placed into an area apparently corresponding to a separate binding cleft located east of the peptide binding region

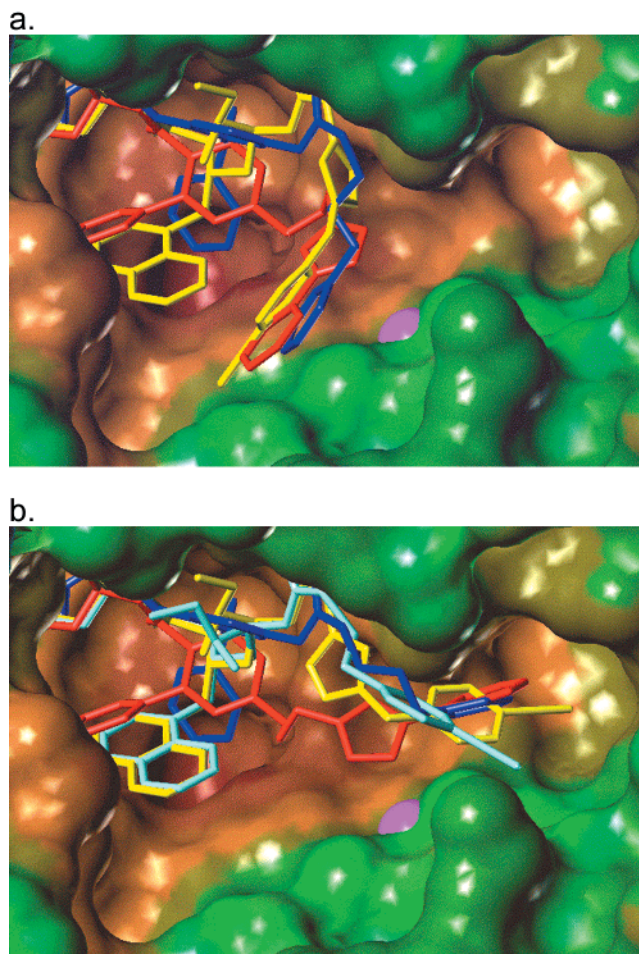


**Figure 2.** (a) Representative solutions of docking runs of compounds **3** (red), **4** (yellow), and **8e** (blue) which orient their terminal aryl residues into close proximity to the hydrophobic surface in the southern hemisphere of the farnesyltransferase's active site. Hydrophobic properties of the enzyme's surface are indicated in brown, hydrophilic in green to blue colors. Enzyme-bound zinc is shown as a magenta sphere. (b) Representative solutions of docking runs of compounds **3** (red), **4** (yellow), **5** (cyan), and **8e** (blue) resulting in an alternative binding mode placing the terminal aryl residues into another separate binding cleft located east of the farnesyltransferase's active site.

and being connected to it via a small channel (Figure 2b). This region ("far binding site") is defined mainly by Tyr 300 $\beta$ , Leu 295 $\beta$ , and three lysine side chains: Lys 294 $\beta$ , Lys 353 $\beta$ , and Lys 356 $\beta$  (Figure 3). Again, the interactions of these larger compounds occur opposite to the phenyl ring of Tyr 300 $\beta$  which appears to be involved in interactions with **1**, **2**, and **8b**. Although it cannot be shown conclusively, we strongly favor the latter, the eastern region, as the second ("far") aryl binding site. In this relatively narrow environment interactions between the aryl moieties of the inhibitors and the amino acid side chains should be more pronounced compared to the southern location where the aryl moiety is located on a rather flat molecular surface and is therefore much more exposed to the aqueous medium than in the eastern cleft. In addition to the flexible docking, we performed GRID searches in the farnesyltransferase's active site and its neighboring regions. Using the "C1=" probe allows to search for locations favorable to interact with aromatic carbons.

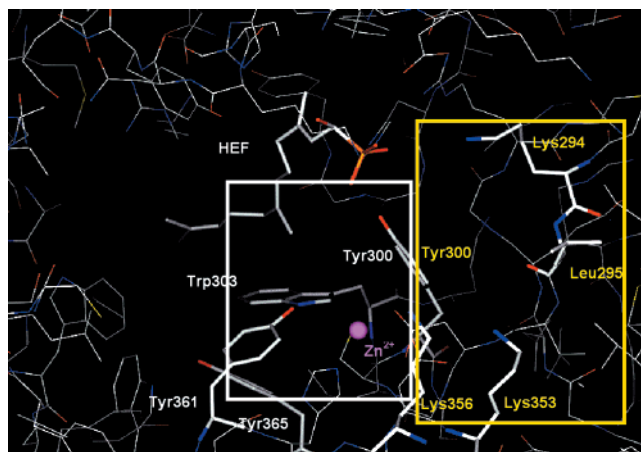


**Figure 3.** Location of the two suggested aryl binding sites (near binding site: white; far binding site: yellow) with the principal amino acid side chains highlighted (HFP:  $\alpha$ -hydroxyfarnesylphosphat, FPP analogue used for the crystal structure). Amino acids belonging to the near binding site are labeled white, those belonging to the far binding site are labeled yellow. Tyr300 belongs to both binding sites.

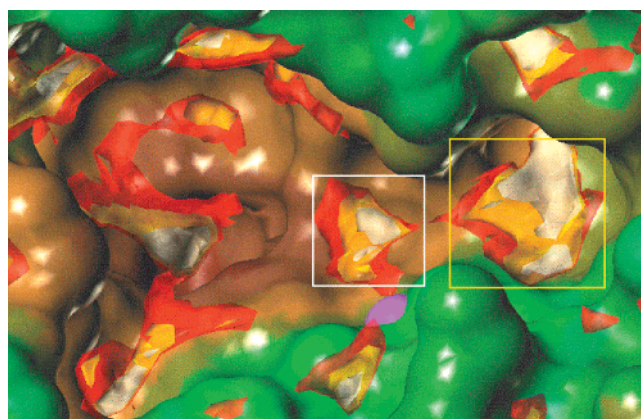


**Figure 4.** Results of the GRID analysis searching for regions favorable for interaction with aryl moieties. The position of the proposed near and far aryl binding sites is indicated in white (near) and yellow (far), respectively. Energy levels:  $-2.25 \text{ kcal mol}^{-1}$ , red;  $-2.75 \text{ kcal mol}^{-1}$ , yellow;  $-3.25 \text{ kcal mol}^{-1}$ , white. Enzyme-bound zinc is shown as a magenta sphere. As can be seen from the yellow and white colored areas, aryl binding is strongly favored in this regions.

As shown in Figure 4, regions favorable for aryl binding are found exactly at the same positions where FlexX has placed the aryl residues of our model compounds. Hence, a second computational method confirmed the results obtained by flexible docking, thus providing further arguments for the reasonableness of our suggestion concerning the location of the postulated aryl binding sites.

In a second step we set out to design some novel non-thiol farnesyltransferase inhibitors based on our benzophenone scaffold which are better suited to fill the novel aryl binding sites than the first model compounds **8a–f**. We decided to first focus our attention on the far aryl binding site. A biaryl structure consisting of a five-membered and a six-membered aromatic ring should be able to fill this far aryl binding site. As a linking structure between this biaryl moiety and our benzophenone scaffold, an acrylic acid structure seemed to be appropriate since it (1) ensures the correct distance between this two partial structures and (2) the trans-

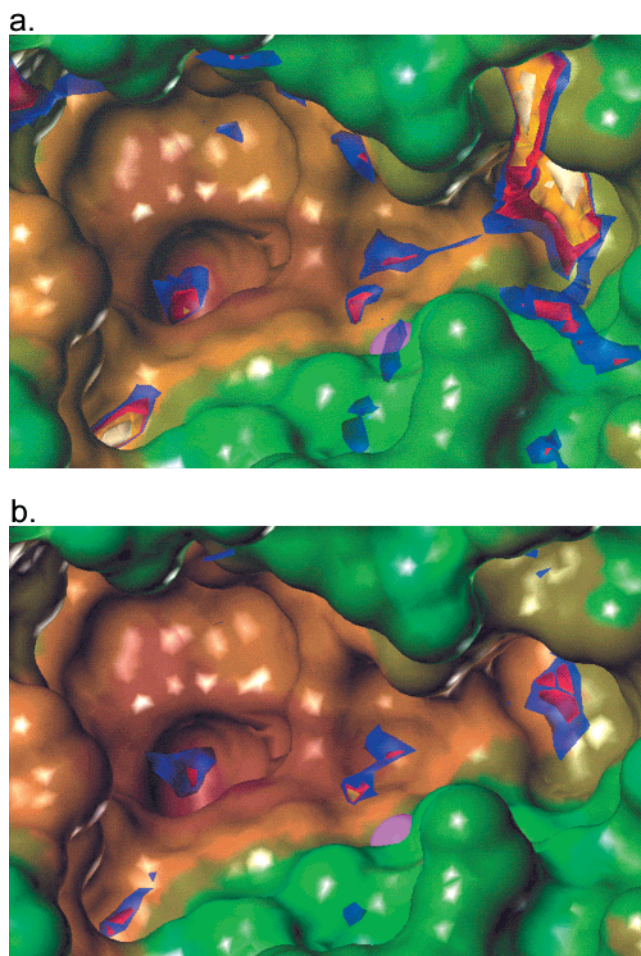


**Figure 5.** Results of the GRID analysis searching for regions favorable for interaction with (a) nitro oxygen and (b) chlorine. Energy levels:  $-5.0 \text{ kcal mol}^{-1}$ , blue;  $-6.0 \text{ kcal mol}^{-1}$ , red;  $-7.0 \text{ kcal mol}^{-1}$ , yellow;  $-8.0 \text{ kcal mol}^{-1}$ , white. Enzyme-bound zinc is shown as a magenta sphere. The proposed far aryl binding site strongly favors the binding of nitro over chlorine.

configured double bond forces the biaryl moiety into the desired direction. To our disappointment, the first biaryl derivative **9a** was only weakly active ( $\text{IC}_{50} = 10.3 \mu\text{M}$ ). However, introduction of a nitro group into the para position of the terminal phenyl (**9b**) resulted in a more than 20-fold improvement in activity ( $\text{IC}_{50} = 455 \text{ nM}$ ). Replacement of the central thiazole by a furan (compound **9c**) resulted in an additional 13-fold improvement in farnesyltransferase inhibitory activity ( $\text{IC}_{50} = 35 \text{ nM}$ ). Replacement of the nitro group by bromine or chlorine (compounds **9d** and **9e**) led to a significant reduction in activity ( $\text{IC}_{50} = 925 \text{ nM}$  and  $\text{IC}_{50} = 6.3 \mu\text{M}$ , respectively). GRID analysis using the "ON" and the "CL" probe searching for regions favorable for binding of nitro and chlorine, respectively, revealed that the proposed far aryl binding site possesses good binding properties for the terminal oxygen of nitro groups (Figure 5a) while binding of chlorine is less favored in this particular region (Figure 5b). These computational results mirror nicely the farnesyltransferase inhibitor activity observed in this first series of inhibitors designed with our binding model in mind. This in turn provides further argument for the correctness of our binding model.

In conclusion, we suggest that the two regions in the farnesyltransferase's active site defined by the side chains of Tyr 300 $\beta$ , Trp 303 $\beta$ , Tyr 361 $\beta$ , and Tyr 365 $\beta$  and by the side chains of Tyr 300 $\beta$ , Leu 295 $\beta$ , Lys 294 $\beta$ , Lys 353 $\beta$ , and Lys 356 $\beta$ , respectively, could be the postulated aryl binding regions. These aryl binding sites may be used for the rational design of non-thiol farnesyltransferase inhibitors as demonstrated with compound **9c**. Our ongoing research is directed toward the establishment of deeper structure–activity relationships of this class of farnesyltransferase inhibitors.

## Experimental Section

<sup>1</sup>H and <sup>13</sup>C NMR spectra were recorded on a JEOL JMN-GX-400 and a JEOL JMN-LA-500 spectrometer. Mass spectra were obtained with a Vacuum Generators VG 7070 H using a Vector 1 data acquisition system from Teknivent or an AutoSpec mass spectrometer from Micromass. IR spectra were recorded on a Nicolet 510P FT-IR spectrometer. Microanalyses were obtained from a CH analyzer according to Dr. Salzer from Labormatic and from a Hewlett-Packard CHN-analyzer type 185. Column chromatography was carried out using silica gel 60 (0.062–0.200 mm) from Merck.

**General Procedure for Preparation of 7 and 8a–f.** 5-Amino-2-tolylacetylaminobenzophenone (**6**) was dissolved in hot toluene (approximately 50 mL), and a solution of 1 equiv of various carbonic acid chlorides in dioxane (approximately 10 mL) was added. The mixtures were heated under reflux for 2 h. Solvent was removed in vacuo to give the crude products.

**N-[3-Benzoyl-4-[(4-methylphenyl)acetylaminophenyl]nicotinoyl amide (7):** from nicotinoyl chloride (0.142 g, 1.0 mmol) and **6** (0.344 g, 1.0 mmol). Purification: chromatographed on silica gel (ethyl acetate:*n*-hexane 3:2) to give a yellow solid: yield 0.099 mg (22%); mp 198 °C; IR (KBr)  $\nu$  3400, 2925, 1675, 1635, 1595, 1555 cm<sup>-1</sup>; <sup>1</sup>H NMR (400 MHz, CDCl<sub>3</sub>)  $\delta$  2.26 (s, 3H), 3.60 (s, 2H), 7.08 (m, 2H), 7.15 (m, 2H), 7.30 (m, 1H), 7.41 (m, 2H), 7.51 (m, 1H), 7.58 (m, 1H), 7.64 (m, 2H), 7.91 (m, 1H), 8.14 (m, 1H), 8.47 (m, 1H), 8.65 (s, 1H), 8.97 (s, 1H), 10.44 (s, 1H); MS (EI)  $m/z$  449 (75, M<sup>+</sup>), 317 (100). Anal. (C<sub>28</sub>H<sub>23</sub>N<sub>3</sub>O<sub>3</sub>) C, H, N.

**N-[3-Benzoyl-4-[(4-methylphenyl)acetylaminophenyl]benzamide (8b):** from benzoyl chloride (0.14 g, 1.0 mmol) and **6** (0.344 g, 1.0 mmol). Purification: recrystallized from toluene to give a yellow solid: yield 0.363 g (81%); mp 212 °C; IR (KBr)  $\nu$  3420, 1650, 1620, 1550, 1500 cm<sup>-1</sup>; <sup>1</sup>H NMR (400 MHz, CDCl<sub>3</sub>)  $\delta$  2.34 (s, 3H), 3.66 (s, 2H), 7.14 (m, 2H), 7.22 (m, 2H), 7.40–7.50 (m, 5H), 7.57 (m, 1H), 7.62 (m, 1H), 7.70 (m, 2H), 7.78 (m, 2H), 7.90 (m, 1H), 7.98 (m, 1H), 8.55 (m, 1H), 10.52 (s, 1H); MS (EI)  $m/z$  448 (96, M<sup>+</sup>), 316 (100). Anal. (C<sub>29</sub>H<sub>24</sub>N<sub>2</sub>O<sub>3</sub>) C, H, N.

**N-[3-Benzoyl-4-[(4-methylphenyl)acetylaminophenyl]-2-phenylacetamide (8b):** from 2-phenyl acetyl chloride (0.2 mL, 1.5 mmol) and **6** (0.516 g, 1.5 mmol). Purification: recrystallized from toluene to give a yellow solid: yield 0.472 g (68%); mp 134 °C; IR (KBr)  $\nu$  3290, 1700, 1670, 1630 cm<sup>-1</sup>; <sup>1</sup>H NMR (400 MHz, CDCl<sub>3</sub>)  $\delta$  2.30 (s, 3H), 3.61 (s, 2H), 3.64 (s, 2H), 7.13 (m, 2H), 7.20 (m, 2H), 7.25–7.45 (m, 6H), 7.57 (m, 1H), 7.43 (m, 2H), 7.55 (m, 1H), 7.65 (m, 2H), 7.87 (m, 1H), 8.43 (m, 1H), 10.44 (s, 1H); MS (EI)  $m/z$  462 (100, M<sup>+</sup>), 330 (79). Anal. (C<sub>30</sub>H<sub>26</sub>N<sub>2</sub>O<sub>3</sub>) C, H, N.

**N-[3-Benzoyl-4-[(4-methylphenyl)acetylaminophenyl]-3-phenylpropionylamide (8c):** from 3-phenylpropionyl chloride (0.17 mL, 1.0 mmol) and **6** (0.344 g, 1.0 mmol). Purification: recrystallized from toluene to give a yellow solid: yield 0.72 g (15%); mp 59 °C; IR (KBr)  $\nu$  3420, 3270, 1655, 1595, 1555, 1505 cm<sup>-1</sup>; <sup>1</sup>H NMR (400 MHz, CDCl<sub>3</sub>)  $\delta$  2.32 (s, 3H), 2.56 (t,  $J$  = 8 Hz, 2H), 2.96 (t,  $J$  = 8 Hz, 2H), 3.66 (s, 2H), 7.14 (m, 5H), 7.22 (m, 5H), 7.35 (m, 1H), 7.47 (m, 2H), 7.58 (m, 1H), 7.66 (m, 2H), 7.75 (m, 1H), 8.44 (m, 1H), 10.47 (s, 1H); MS (EI)  $m/z$  476 (57, M<sup>+</sup>), 458 (100). Anal. (C<sub>31</sub>H<sub>28</sub>N<sub>2</sub>O<sub>3</sub>) C, H, N.

**N-[3-Benzoyl-4-[(4-methylphenyl)acetylaminophenyl]-4-phenylbutyryl amide (8d):** from 4-phenylbutyryl chloride (0.185 mg, 1.0 mmol) and **6** (0.344 g, 1.0 mmol). Purification: chromatographed on silica gel (ethyl acetate:*n*-hexane 2:3) to give a yellow solid: yield 0.407 g (83%); mp 117 °C; IR (KBr)  $\nu$  3430, 3290, 2945, 1700, 1645 cm<sup>-1</sup>; <sup>1</sup>H NMR (400 MHz, CDCl<sub>3</sub>)  $\delta$  1.94 (m, 2H), 2.20 (m, 2H), 2.26 (s, 3H), 2.60 (m, 2H), 3.60 (s, 2H), 7.10 (m, 5H), 7.17 (m, 5H), 7.41 (m, 3H), 7.53 (m, 1H), 7.61 (m, 2H), 7.72 (m, 1H), 8.44 (m, 1H), 10.41 (s, 1H); MS (EI)  $m/z$  490 (100, M<sup>+</sup>), 358 (52). Anal. (C<sub>32</sub>H<sub>30</sub>N<sub>2</sub>O<sub>3</sub>) C, H, N.

**N-[3-Benzoyl-4-[(4-methylphenyl)acetylaminophenyl]-5-phenylvaleryl amide (8e):** from 5-phenylvaleryl chloride (0.200 g, 1.0 mmol) and **6** (0.344 g, 1.0 mmol). Purification: chromatographed on silica gel (ethyl acetate:*n*-hexane 2:3) to give a yellow solid: yield 0.247 g (49%); mp 126 °C; IR  $\nu$  3433, 3262, 2932, 1657, 1560, 1504 cm<sup>-1</sup>; <sup>1</sup>H NMR (400 MHz, CDCl<sub>3</sub>)  $\delta$  1.61 (m, 4H), 2.21 (m, 2H), 2.26 (s, 3H), 2.55 (m, 2H), 3.60 (s, 2H), 7.09 (m, 5H), 7.18 (m, 5H), 7.40 (m, 3H), 7.51 (m, 1H), 7.62 (m, 2H), 7.76 (m, 1H), 8.41 (m, 1H), 10.41 (s, 1H); MS (EI)  $m/z$  504 (50, M<sup>+</sup>), 212 (100), 105 (68). Anal. (C<sub>33</sub>H<sub>32</sub>N<sub>2</sub>O<sub>3</sub>) C, H, N.

**N-[3-Benzoyl-4-[(4-methylphenyl)acetylaminophenyl]-6-phenylhexanoyl amide (8f):** from 6-phenylhexanoyl chloride (0.190 g, 1.0 mmol) and **6** (0.344 g, 1.0 mmol). Purification: recrystallized from toluene to give a yellow solid: yield 0.186 g (36%); mp 75 °C; IR (KBr)  $\nu$  3268, 2930, 1666, 1596, 1506 cm<sup>-1</sup>; <sup>1</sup>H NMR (500 MHz, CDCl<sub>3</sub>)  $\delta$  1.35 (m, 2H), 1.62 (m, 2H), 1.68 (m, 2H), 2.26 (m, 2H), 2.33 (s, 3H), 2.58 (m, 2H), 3.69 (s, 2H), 7.14 (m, 5H), 7.24 (m, 5H), 7.48 (m, 3H), 7.58 (m, 1H), 7.69 (m, 2H), 7.83 (m, 1H), 8.50 (m, 1H), 10.47 (s, 1H); MS (EI)  $m/z$  518 (42, M<sup>+</sup>), 105 (100), 91 (99). Anal. (C<sub>34</sub>H<sub>34</sub>N<sub>2</sub>O<sub>3</sub>) C, H, N.

**N-[3-Benzoyl-4-[(4-methylphenyl)acetylaminophenyl]-3-(2-phenyl-4-thiazoly)acrylic acid amide (9a):** from 3-(2-phenyl-4-thiazoly)acrylic acid chloride (0.3 g, 1.2 mmol) and **6** (0.413 g, 1.2 mmol). Purification: recrystallized from toluene to give a yellow solid: yield: 0.394 g (59%); mp 183 °C; IR (KBr)  $\nu$  3345, 3270, 3075, 1680, 1660, 1655, 1595, 1550 cm<sup>-1</sup>. <sup>1</sup>H NMR (400 MHz, CDCl<sub>3</sub>)  $\delta$  2.32, (s, 3H), 3.69, (s, 2H), 6.99 (d,  $J$  = 16 Hz, 1H), 7.14–7.16 (m, 2H), 7.23–7.25 (m, 2H), 7.31–7.32 (m, 1H), 7.39–7.48 (m, 5H), 7.54–7.61 (m, 3H), 7.69–7.71 (m, 2H), 7.84 (s, br, 1H), 7.90–7.93 (m, 2H), 8.03 (s, br, 1H), 8.51 (d,  $J$  = 9 Hz, 1H), 10.52 (s, br, 1H); MS  $m/z$  (%) 557 (96) [M<sup>+</sup>], 558 (37), 452 (21), 425 (21), 344 (27), 214 (100), 212 (24). Anal. (C<sub>34</sub>H<sub>27</sub>N<sub>3</sub>O<sub>5</sub>S) C, H, N, S.

**N-[3-Benzoyl-4-[(4-methylphenyl)acetylaminophenyl]-3-[2-(4-nitrophenyl)-4-thiazoly]acrylic acid amide (9b):** From 3-[2-(4-nitrophenyl)-4-thiazoly]acrylic acid chloride (0.354 g, 1.2 mmol) and **6** (0.413 g, 1.2 mmol). Purification: MPLC EtOAc:*n*-hexane 2:1 to give a yellow solid: yield 0.376 g (52%); mp 243 °C; IR (KBr)  $\nu$  3335, 3085, 2920, 1685, 1660, 1635, 1595, 1550, 1515 cm<sup>-1</sup>; <sup>1</sup>H NMR (500 MHz, CDCl<sub>3</sub>)  $\delta$  2.34, (s, 3H), 3.71, (s, 2H), 7.01 (d,  $J$  = 16 Hz, 1H), 7.17–7.18 (m, 2H), 7.24–7.28 (m, 4H), 7.44–7.54 (m, 3H), 7.59–7.68 (m, 2H), 7.72–7.74 (m, 2H), 8.00 (s, br, 1H), 8.12–8.14 (m, 2H), 8.28–8.32 (m, 2H), 8.57–8.59 (m, 1H), 10.54 (s, br, 1H); MS  $m/z$  (%) 602 (5) [M<sup>+</sup>], 345 (17), 344 (79), 259 (14), 239 (20), 238 (13), 213 (22), 212 (100), 211 (47), 142 (13), 105 (42), 44 (11), 40 (24). Anal. (C<sub>34</sub>H<sub>26</sub>N<sub>4</sub>O<sub>5</sub>S) C, H, N, S.

**N-[3-Benzoyl-4-[(4-methylphenyl)acetylaminophenyl]-3-[5-(4-nitrophenyl)-2-furyl]acrylic acid amide (9c):** From 3-[5-(4-nitrophenyl)-2-furyl]acrylic acid chloride (0.333 g, 1.2 mmol) and **6** (0.413 g, 1.2 mmol). Purification: MPLC EtOAc:*n*-hexane 1:1 to give a yellow solid: yield 0.311 g (48%); mp 221 °C; IR (KBr)  $\nu$  3260, 2920, 1665, 1630, 1595, 1550, 1510 cm<sup>-1</sup>; <sup>1</sup>H NMR (500 MHz, CDCl<sub>3</sub>)  $\delta$  2.33, (s, 3H), 3.69, (s, 2H), 6.59 (d,  $J$  = 15 Hz, 1H), 6.67–6.68 (m, 1H), 6.90–6.91 (m, 1H), 7.15–7.17 (m, 2H), 7.23–7.25 (m, 2H), 7.45–7.48 (m, 3H), 7.56–7.59 (m, 1H), 7.61–7.64 (m, 1H), 7.70–7.71 (m, 2H), 7.76 (d,  $J$  = 8.8 Hz, 2H), 7.93 (s, br, 1H), 8.03 (s, br, 1H), 8.20 (d,  $J$  = 8.8 Hz, 2H), 8.51 (d,  $J$  = 9 Hz, 1H), 10.52 (s, br, 1H); MS  $m/z$  (%) 585 (52) [M<sup>+</sup>], 583 (15), 453 (18), 345 (17), 344 (71),

326 (18), 325 (20), 243 (15), 242 (100), 238 (15), 212 (80), 211 (29), 196 (22), 105 (39), 40 (11). Anal. (C<sub>35</sub>H<sub>27</sub>N<sub>3</sub>O<sub>6</sub>): C, H, N.

**N-[3-Benzoyl-4-[(4-methylphenyl)acetylaminophenyl]-3-[5-(4-bromophenyl)-2-furyl]acrylic acid amide (9d):** from 3-[5-(4-bromophenyl)-2-furyl]acrylic acid chloride (0.355 g, 1.2 mmol) and **6** (0.413 g, 1.2 mmol). Purification: MPLC EtOAc:*n*-hexane 1:1 to give a yellow solid: yield 0.468 g (63%); mp 237 °C; IR (KBr)  $\nu$  3300, 3045, 2360, 1685, 1660, 1635, 1595, 1550, 1505 cm<sup>-1</sup>; <sup>1</sup>H NMR (500 MHz, CDCl<sub>3</sub>)  $\delta$  2.33, (s, 3H), 3.68, (s, 2H), 6.43 (d, *J* = 15 Hz, 1H), 6.62–6.64 (m, 1H), 6.68–6.70 (m, 1H), 7.13–7.16 (m, 2H), 7.21–7.25 (m, 3H), 7.30 (s, br, 1H), 7.42–7.62 (m, 8H), 7.71–7.72 (m, 2H), 7.94 (s, br, 1H), 8.54 (d, *J* = 9 Hz, 1H), 10.46 (s, br, 1H); MS *m/z* (%) 620 (34) [M<sup>+</sup> + 2], 618 (26) [M<sup>+</sup>], 607 (26), 344 (44), 277 (100), 275 (88), 265 (40), 212 (24), 105 (23), 40 (46). Anal. (C<sub>35</sub>H<sub>27</sub>BrN<sub>2</sub>O<sub>4</sub>): C, H, Br, N.

**N-[3-Benzoyl-4-[(4-methylphenyl)acetylaminophenyl]-3-[5-(4-chlorophenyl)-2-furyl]acrylic acid amide (9e):** from 3-[5-(4-chlorophenyl)-2-furyl]acrylic acid chloride (0.321 g, 1.2 mmol) and **6** (0.413 g, 1.2 mmol). Purification: MPLC EtOAc:*n*-hexane 1:1 to give a yellow solid: yield 0.493 g (71%); mp 240 °C; IR (KBr)  $\nu$  3320, 1685, 1660, 1635, 1595, 1555, 1505 cm<sup>-1</sup>; <sup>1</sup>H NMR (500 MHz, DMSO-*d*<sub>6</sub>)  $\delta$  2.26, (s, 3H), 3.38, (s, 2H), 6.70 (d, *J* = 15 Hz, 1H), 6.94–6.95 (m, 1H), 7.00–7.02 (m, 2H), 7.04–7.06 (m, 2H), 7.12–7.13 (m, 1H), 7.38 (d, *J* = 15 Hz, 1H), 7.48–7.55 (m, 4H), 7.62–7.65 (m, 2H), 7.69–7.70 (m, 2H), 7.77–7.79 (m, 3H), 7.88–7.90 (m, 1H), 10.03 (s, br, 1H), 10.30 (s, br, 1H); MS *m/z* (%) 576 (29) [M<sup>+</sup> + 2], 574 (72) [M<sup>+</sup>], 345 (12), 344 (48), 233 (33), 232 (15), 231 (100), 212 (16). Anal. (C<sub>35</sub>H<sub>27</sub>ClN<sub>2</sub>O<sub>4</sub>): C, H, Cl, N.

**Enzyme Preparation.** Yeast farnesyltransferase was used as a fusion to glutathione S-transferase at the N-terminus of the  $\beta$ -subunit. Farnesyltransferase was expressed in *Escherichia coli* DH5 $\alpha$  grown in LB media containing ampicillin and chloramphenicol for coexpression of pGEX-DPR1 and pBC-RAM2 for farnesyltransferase production.<sup>27</sup> The enzyme was purified by standard procedures with glutathione-agarose beads for selective binding of the target protein.

**Farnesyltransferase Assay.** The assay was conducted as described elsewhere.<sup>28</sup> Farnesylpyrophosphate (FPP) was obtained as a solution of the ammonium salt in methanol-10 mM aqueous NH<sub>4</sub>Cl (7:3) from Sigma-Aldrich. Dansyl-GlyCys-ValLeuSer (Ds-GCVLS) was custom synthesized by ZMBH, Heidelberg, Germany. The assay mixture (100  $\mu$ L volume) contained 50 mM Tris/HCl pH 7.4, 5 mM MgCl<sub>2</sub>, 10  $\mu$ M ZnCl<sub>2</sub>, 5 mM dithiothreitol (DTT), 7  $\mu$ M Ds-GCVLS, 20  $\mu$ M FPP, and 5 nmol (approximately) yeast GST-farnesyltransferase and 1% of various concentrations of the test compounds dissolved in dimethyl sulfoxide (DMSO). The progress of the enzyme reaction was followed by monitoring the enhancement of the fluorescence emission at 505 nm (excitation 340 nm). The reaction was started by addition of the enzyme and run in a Quartz cuvette thermostated at 30 °C. Fluorescence emission was recorded with a Perkin-Elmer LS50B spectrometer. IC<sub>50</sub> values (concentrations resulting in 50% inhibition) were calculated from initial velocity of three independent measurements of four to five different concentrations of inhibitor.

**Molecular Modeling.** All molecular modeling was carried out using SYBYL<sup>21</sup> version 6.6/6.7 running on a Silicon Graphics O2 (R10000). Flexible docking was performed using FlexX<sup>20</sup> version 1.7.6. The FlexX command MAPREF and the perturbate mode of the PLACEBAS command were used. Default parameters were employed except the MAX\_ENERGY value which was set to 10 kJ mol<sup>-1</sup>. GRID<sup>25</sup> (version 19) analyses were realized using a grid box with dimensions of 22 Å  $\times$  30 Å  $\times$  20 Å. A grid spacing of 0.5 Å was used to get a detailed description of the binding region and to retrieve smooth contour maps better for interpretation.

**Acknowledgment.** The authors gratefully thank Prof. Dr. G. Klebe who provided us with all facilities needed for the modeling and also for helpful discussions. The pGEX-DPR1 and pBC-RAM2 plasmids were kindly provided by Prof. F. Tamanoi (UCLA). I.S. thanks Prof.

Dr. S. Grabley and PD Dr. R. Thiericke for generous support and Ms. S. Egner for excellent technical assistance. Financial support by the German Pharmaceutical Society is gratefully acknowledged.

## References

- Leonard, D. M. Ras Farnesyltransferase: A New Therapeutic Target. *J. Med. Chem.* **1997**, *40*, 2971–2990.
- Qian, Y.; Sebti, S. M.; Hamilton, A. D. Farnesyltransferase as a Target for Anticancer Drug Design. *Biopolymers* **1997**, *43*, 25–41.
- Sebti, S. M.; Hamilton, A. D. New approaches to anticancer drug design based on the inhibition of farnesyltransferase. *Drug Discovery Today* **1998**, *3*, 26–32.
- Zhang, F. L.; Casey, P. J. Protein Prenylation: Molecular Mechanism and Functional Consequences. *Annu. Rev. Biochem.* **1996**, *65*, 241–269.
- Cox, A. D.; Der, C. J. Farnesyltransferase inhibitors and cancer treatment: targeting simply Ras? *Biochim. Biophys. Acta* **1997**, *1333*, F51–F71.
- Du, W.; Lebowitz, P. F.; Prendergast, G. C. Cell Growth Inhibition by Farnesyltransferase Inhibitors Is Mediated by Gain of Geranylgeranylated RhoB. *Mol. Cell. Biol.* **1999**, *19*, 1831–1840.
- Prendergast, G. C. Farnesyltransferase inhibitors: antineoplastic mechanism and clinical prospects. *Curr. Opin. Cell Biol.* **2000**, *12*, 166–173.
- Oliff, A. Farnesyltransferase inhibitors: targeting the molecular basis of cancer. *Biochim. Biophys. Acta* **1999**, *1423*, C19–C30.
- Strickland, C. L.; Windsor, W. T.; Syto, R.; Wang, L.; Bond, R.; Wu, R.; Schwartz, J.; Le, H. V.; Beese, L. S.; Weber, P. C. Crystal Structure of Farnesyl Protein Transferase Complexed with a CaaX peptide and Farnesyl Diphosphate Analogue. *Biochemistry* **1998**, *37*, 16601–16611.
- Martindale *The Extra Pharmacopeia*, 31st ed.; Reynolds, J. E. F., Ed.; Royal Pharmaceutical Society of Great Britain: London, 1996; p 821.
- Hunt, J. T.; Lee, V. G.; Leftheris, K.; Seizinger, B.; Carboni, J.; Mabus, J.; Ricca, C.; Yan, N.; Manne, V. Potent, Cell Active Non-Thiol Tetrapeptide Inhibitors of Farnesyltransferase. *J. Med. Chem.* **1996**, *39*, 353–358.
- O'Connor, S. J.; Barr, K. J.; Wang, L.; Sorensen, B. K.; Tasker, A. S.; Sham, H.; Ng, A.-C.; Cohen, J.; Devine, E.; Cherian, S.; Saeed, B.; Zhang, H.; Lee, J. Y.; Warner, R.; Tahir, S.; Kovar, P.; Ewing, P.; Alder, J.; Mitten, M.; Leal, J.; Marsh, K.; Bauch, J.; Hoffman, D. J.; Sebti, S. M.; Rosenberg, S. H. Second-Generation Peptidomimetic Inhibitors of Protein Farnesyltransferase Demonstrating Improved Cellular Potency and Significant *In Vivo* Efficacy. *J. Med. Chem.* **1999**, *42*, 3701–3710.
- Augeri, D. J.; Janowick, D.; Kalvin, D.; Sullivan, G.; Larsen, J.; Dickman, D.; Ding, H.; Cohen, J.; Lee, J.; Warner, R.; Kovar, P.; Cherian, S.; Saeed, B.; Zhang, H.; Tahir, S.; Ng, S.-C.; Sham, H.; Rosenberg, S. H. Potent and Orally Bioavailable Nonycysteine-Containing Inhibitors of Protein Farnesyltransferase. *Bioorg. Med. Chem. Lett.* **1999**, *9*, 1069–1074.
- Breslin, M. J.; deSolms, J.; Giuliani, E. A.; Stokker, G. E.; Graham, S. L.; Pompliano, D. L.; Mosser, S. D.; Hamilton, K. A.; Hutchinson, J. H. Potent, Non-Thiol Inhibitors of Farnesyltransferase. *Bioorg. Med. Chem. Lett.* **1998**, *8*, 3311–3316.
- Ciccarone, T. M.; MacTough, S. C.; Williams, T. M.; Dinsmore, C. J.; O'Neill, T. J.; Shah, D.; Culbertson, J. C.; Koblan, K. S.; Kohl, N. E.; Gibbs, J. B.; Oliff, A. I.; Graham, S. L.; Hartman, G. D. Non-Thiol 3-Aminomethylbenzamide Inhibitors of Farnesyl-protein Transferase. *Bioorg. Med. Chem. Lett.* **1999**, *9*, 1991–1996.
- Anthony, N. J.; Gomez, R. P.; Schaber, M. D.; Mosser, S. D.; Hamilton, K. A.; O'Neill, T. J.; Koblan, K. S.; Graham, S. L.; Hartman, G. D.; Shah, D.; Rands, E.; Kohl, N. E.; Gibbs, J. B.; Oliff, A. I. Design and *In Vivo* Analysis of Potent Non-Thiol Inhibitors of Farnesyl Protein Transferase. *J. Med. Chem.* **1999**, *42*, 3356–3368.
- Schlitzer, M.; Sattler, I.; Dahse, H.-M. Different Amino Acid Replacements in CAAX-Tetrapeptide Based Farnesyltransferase Inhibitors. *Arch. Pharm. Pharm. Med. Chem.* **1999**, *332*, 124–132.
- Sakowski, J.; Böhm, M.; Sattler, I.; Dahse, H.-M.; Schlitzer, M. Synthesis, Molecular Modeling and Structure Activity Relationship of Benzophenone-Based CAAX-Peptidomimetic Farnesyltransferase Inhibitors. Submitted.
- Schlitzer, M.; Sattler, I. Non-Thiol Farnesyltransferase Inhibitors: the concept of benzophenone-based bisubstrate analogue farnesyltransferase inhibitors. *Eur. J. Med. Chem.* **2000**, *35*, 721–726.
- Rarey, M.; Kramer, B.; Lengauer, T.; Klebe, G. A fast flexible docking method using an incremental construction algorithm. *J. Mol. Biol.* **1996**, *261*, 470–489.

- (21) SYBYL molecular modeling software; Tripos Inc.: 1699 South Hanley Rd, Suite 303, St. Louis, MO 63144.
- (22) Goodford, P. J. A computational procedure for determining energetically favorable binding sites on biologically important macromolecules. *J. Med. Chem.* **1985**, *28*, 849–857.
- (23) Boobbyer, D. N.; Goodford, P. J.; McWhinnie, P. M.; Wade, R. C. New hydrogen-bond potentials for use in determining energetically favorable binding sites on molecules of known structure. *J. Med. Chem.* **1989**, *32*, 1083–1094.
- (24) Wade, R. C.; Clark, K. J.; Goodford, P. J. Further development of hydrogen bond functions for use in determining energetically favorable binding sites on molecules of known structure. 1. Ligand probe groups with the ability to form two hydrogen bonds. *J. Med. Chem.* **1993**, *36*, 140–147. Wade, R. C.; Goodford, P. J. Further development of hydrogen bond functions for use in determining energetically favorable binding sites on molecules of known structure. 2. Ligand probe groups with the ability to form more than two hydrogen bonds. *J. Med. Chem.* **1993**, *36*, 148–156.
- (25) GRID, version 19; Molecular Discovery Ltd.: West Way House, Elms Parade, Oxford, U.K.
- (26) Augeri, D. J.; O'Conner, S. J.; Janowick, D.; Szczepankiewicz, B.; Sullivan, G.; Larsen, J.; Kalvin, D.; Cohen, J.; Devine, E.; Zhang, H.; Cherian, S.; Saeed, B.; Ng, S.-C.; Rosenberg, S. Potent and Selective Non-Cysteine-Containing Inhibitors of Protein Farnesyltransferase. *J. Med. Chem.* **1998**, *41*, 4288–4300.
- (27) Del Villar, K.; Mitsuzawa, H.; Yang, W.; Sattler, I.; Tamanoi, F. Amino Acid Substitutions That Convert the Protein Substrate Specificity of Farnesyltransferase to That of Geranylgeranyltransferase Type I. *J. Biol. Chem.* **1997**, *272*, 680–687.
- (28) Pompliano, D. L.; Gomez, R. P.; Anthony, N. J. Intramolecular Fluorescence Enhancement: A Continuous Assay of Ras Farnesyl:Protein Transferase. *J. Am. Chem. Soc.* **1992**, *114*, 7945–7946.

JM010873J